

Thin-cap fibroatheroma and increased coronary intima-media thickness are associated with an altered balance of arginine metabolites

Patrycja Mołek^{1,2}, Paweł Żmudzki³, Andrzej Machnik⁴, Grażyna Nowak⁴,
Konrad Stępień^{1,2}, Mateusz Wnuk², Aleksandra Włodarczyk¹, Karol Nowak¹,
Radosław Rychlak², Jadwiga Nessler^{1,2}, Jarosław Zalewski^{1,2}

1 Department of Coronary Disease and Heart Failure, Jagiellonian University Medical College, Kraków, Poland

2 Clinical Department of Coronary Disease and Heart Failure, John Paul II Hospital, Kraków, Poland

3 Faculty of Pharmacy, Jagiellonian University Medical College, Kraków, Poland

4 Clinical Department of Interventional Cardiology, John Paul II Hospital, Kraków, Poland

KEY WORDS

arginine,
atherosclerosis,
metabolism,
myocardial infarction,
optical coherence
tomography

EDITORIAL

by [Tsikas and Büttner](#)

ABSTRACT

INTRODUCTION Arginase inhibition increases plasma citrulline and citrulline/ornithine (C/O) ratio, and reduces plasma ornithine and ornithine/arginine (O/A) ratio in an animal model of myocardial infarction (MI). **OBJECTIVES** We hypothesized that the presence of thin-cap fibroatheroma (TCFA) in the culprit lesion and increased non-culprit intima-media thickness of an infarct-related artery (IRA) are associated with an altered balance of arginine metabolites.

PATIENTS AND METHODS Arginine and its metabolites were measured using liquid chromatography and tandem mass spectrometry in 100 consecutive MI patients upon admission and at 6-month follow-up. TCFA and adjacent to culprit lesion proximal and distal 10-mm segments were assessed with optical coherence tomography in the acute phase. Twenty five patients without coronary lesions on angiography served as controls.

RESULTS The C/O ratio increased 5.33 times ($P < 0.001$), while the O/A ratio decreased 2.53 times ($P < 0.001$) at the 6-month follow-up, as compared with the acute phase of MI. The patients with ($n = 75$) vs without ($n = 25$) TCFA had lower C/O ratio by 29% ($P = 0.003$), while the mean intima-media diameter of adjacent non-culprit region correlated with the follow-up O/A ratio ($R = 0.337$; $P = 0.003$). In a multivariable analysis, a higher acute phase C/O ratio was associated with a lower risk of TCFA presence (odds ratio, 0.978; 95% CI, 0.962–0.994; $P = 0.006$), whereas a higher follow-up O/A ratio correlated with larger intima-media diameter of the adjacent segments (β coefficient, 0.227; 95% CI for β coefficient, 0.045–0.409; $P = 0.018$).

CONCLUSIONS Enhanced arginase activity over nitric oxide synthase following ischemia was associated with the presence of TCFA in the culprit lesion, while a similar metabolic shift in the chronic phase correlated with a greater thickness of the intima-media in the adjacent non-culprit IRA segments.

INTRODUCTION Endothelial dysfunction is identified by an impaired endogenous vasorelaxant ability associated mainly with uncoupling of endothelial nitric oxide synthase (NOS).^{1,2} At every stage of the atherosclerotic plaque remodeling, formation of a fibrous cap overlying the lipid necrotic core, which is prone to rupture and to trigger thrombus generation,

may occur. In an intact endothelial lining, NOS metabolizes L-arginine to L-citrulline and nitric oxide (NO). On the other hand, L-arginine can be competitively catalyzed to L-ornithine by arginase, an enzyme participating in the final step of the urea cycle.³⁻⁵ Thus, the metabolic competition of both enzymes for L-arginine may potentially contribute to the thin-cap

Correspondence to:

Jarosław Zalewski, MD, PhD,
Department of Coronary Disease and
Heart Failure, Jagiellonian University
Medical College, ul. Piłsudskiego 80,
31-202 Kraków, Poland,
phone: +48 126142218,
email: jzalewski@szpitaljp2.krakow.pl
Received: September 13, 2022.
Revision accepted: October 6, 2022.
Published online: October 13, 2022.
Pol Arch Intern Med. 2023;
133 (2): 16356
doi:10.20452/pamw.16356
Copyright by the Author(s), 2023

WHAT'S NEW?

Nitric oxide synthase (NOS) produces a potent signaling molecule nitric oxide. Arginase, by competing with NOS for the same substrate, that is, arginine, reduces nitric oxide production. This study demonstrates that during the acute phase of myocardial infarction arginine metabolism is shifted toward arginase over NOS. An enhanced arginase activity in the acute setting is associated with the presence of the features of unstable coronary plaque responsible for acute coronary syndromes expressed as thin-cap fibroatheroma. In turn, a similar residual metabolic shift toward arginase in the chronic phase correlates with a greater thickness of the intima-media in the stable segments of the infarct-related artery. This study shows that arginine metabolites and their derivatives might be considered new, noninvasive indicators useful in identification of patients who are more likely to have vulnerable plaque as well as in monitoring the extent of chronic atherosclerotic lesions.

fibroatheroma (TCFA) formation or coronary plaque remodeling.

Several lines of evidence indicate that different biomarkers or their ratios might be useful in cardiovascular prognosis after myocardial infarction (MI).⁵⁻⁸ Atherogenic lipoproteins, mainly low-density lipoprotein (LDL) cholesterol, initiate atherosclerosis by depositing in the arterial intima⁹ and promote arterial wall inflammation.¹⁰ This systemic inflammatory response can be measured by assessing the level of high-sensitivity C-reactive protein (hsCRP), which is strongly associated with cardiovascular risk.^{11,12} Other biomarkers, including acid-base balance parameters,¹³ apolipoprotein-associated phospholipase A2,¹⁴ matrix metalloproteinases 2 and 9,¹⁵ myeloperoxidase,¹⁶ and oxidized LDL¹⁰ were found to be associated with the plaque instability in acute coronary syndromes. Nevertheless, none of those mediators or biomarkers are clinically effective to trace the process of endothelial dysfunction followed by asymptomatic atherosclerosis or to predict the plaque vulnerability associated with acute adverse cardiovascular events.

TCFA with the lipid necrotic core covered by a thin (<65 µm) fibrous intima layer is identified in 50% to 75% of MI patients.¹⁷⁻¹⁹ In vivo serial intravascular imaging studies indicate that LDL cholesterol-lowering therapy with statins^{20,21} or proprotein convertase subtilisin/kexin type 9 inhibitor^{22,23} within 6 to 12 months dynamically increases a minimum fibrous cap thickness by 25% to 300%, reduces lipid content by 18% to 21% and macrophage infiltration by 15% to 32%, thus stabilizing the culprit lesion. In contrast, the same drugs reduce the volume of a stable coronary plaque at most by 0.9% to 2.2% within 9 to 12 months.²³⁻²⁵ On the other hand, experimental studies provide evidence that systemic arginase inhibition during myocardial ischemia and reperfusion is associated with changes in the balance of arginine metabolites,²⁶ but their relationships with morphology of the infarct-related artery (IRA) remain poorly understood.

Thus, we sought to investigate whereas the presence of TCFA in the culprit vulnerable lesion and increased intima-media thickness in the adjacent to culprit segments with stable lesions are associated with an altered balance of arginine metabolites following MI.

PATIENTS AND METHODS **Patients** Between January 2018 and June 2021, we enrolled 100 Caucasian patients aged at least 18 years with an ST-segment elevation MI (STEMI), who underwent primary percutaneous coronary intervention (PCI). The inclusion criteria were chest pain lasting no more than 12 hours at rest with an accompanying ST-segment elevation above 1 mm in 2 or more limb leads, or above 2 mm in 2 or more precordial leads, or a new left bundle branch block. The exclusion criteria were a lack of informed consent, cardiogenic shock or pulmonary edema, history of MI or PCI at the same location or coronary artery bypass surgery, history of cancer, venous thromboembolism, renal failure with glomerular filtration rate below 30 ml/min/1.73 m², liver failure with bilirubin level above 2 mg/dl and/or spontaneous international normalized ratio above 2, or contraindications to optical coherence tomography (OCT) imaging. The controls were 25 patients with chronic coronary syndrome, similar to the MI group in terms of demographics, cardiovascular risk factors, and comorbidities. The control patients had no coronary lesions on angiography despite positive stress tests for ischemia. The demographic characteristics, cardiovascular risk factors, history of cardiovascular diseases, and comorbidities were collected for all the patients. Upon admission, hemoglobin (reference range [RR], 11.2–15.7 g/dl), hematocrit (RR, 34.1%–44.9%), red (RR, 3.98–10.4 × 10³/µl) and white (RR, 3.93–5.22 × 10⁶/µl) blood cell count, platelet count (RR, 140–440 × 10³/µl), lipid profile, glucose, creatinine (RR, 62–106 µmol/l), hsCRP (RR, <3.0 mg/l) and fibrinogen (RR, 2.1–4.0 g/l) were determined using standard laboratory techniques. Serum activity of isoenzyme MB of creatine kinase (CK-MB; RR, 0–24 IU/l), as well as concentration of cardiac high-sensitivity troponin T (RR, <0.014 ng/ml) were measured upon admission, and then subsequently every 12 hours over the first 48 hours. Diabetes mellitus (DM) was established based on either a fasting glycemic level equal to or greater than 7 mmol/l on 2 separate occasions or the use of hypoglycemic drugs. Diagnosis of a prior ischemic stroke was based on a clinical presentation and positive computed tomography or magnetic resonance imaging findings. Dyslipidemia was established based on either the administration of lipid-lowering therapy or when lipid levels were elevated above 5 mmol/l for total cholesterol or 2.6 mmol/l for LDL cholesterol.

The study was approved by the Ethics Committee of the Jagiellonian University (122.6120.61.2016), and all the procedures were performed in

accordance with relevant guidelines and regulations. All the study participants provided a written informed consent prior to their inclusion to the study.

Quantification of arginine metabolites The quantification of arginine metabolites was performed as previously described.²⁷ Briefly, blood samples were drawn into citrate tubes upon admission in the acute phase of MI, and again 6 months later. The samples were centrifuged at 2500 g at 18 °C to 22 °C for 20 minutes and processed immediately or stored in aliquots at -80 °C until analysis. Plasma proteins for amino acid analysis were precipitated before measurement with 80% methanol. The concentrations of arginine, ornithine, citrulline, proline, spermidine, agmatine, asymmetric dimethylarginine (ADMA), and monomethyl arginine (MMA) were measured in duplicate by ultra-performance liquid chromatography-tandem mass spectrometry (UPLC-MS/MS) using a Waters ACQUITY UPLC (Waters Corporation, Milford, Massachusetts, United States) coupled to a Waters TQD mass spectrometer (electrospray ionization mode electrospray ionization-tandem quadrupole).

Chromatographic separation of amino acids was carried out using the Acquity UPLC BEH Amide column, 2.1 mm × 100 mm, and the 1.7 μm particle size equipped with a VanGuard Acquity UPLC BEH Amide pre-column (Waters Corporation, Milford, Massachusetts, United States). The column was maintained at 40 °C and eluted under linear gradient elution from 20% to 35% of eluent A over 4 minutes, followed by linear gradient elution from 35% to 40% of eluent A over 6 minutes, with a flow rate of 0.3 ml/min. Eluent A was water / formic acid (0.1%, v/v), and eluent B was acetonitrile / formic acid (0.1%, v/v).

The Waters TQD mass spectrometer parameters were optimized for quantitative analysis using the solutions of L-arginine, N^G, N^G-dimethylarginine, L-citrulline, L-ornithine, L-proline, 4-((4-((2-aminoethyl)amino)naphthalen-1-yl)diazenyl)benzenesulfonamide, and chloramphenicol, at 10 μg/ml, at a flow rate of 20 μl/min, and a 1:1 (v/v) mixture of eluents A and B at a flow rate of 0.28 ml/min.

Global arginine bioavailability ratio (GABR) was calculated as arginine level divided by the sum of concentrations of ornithine and citrulline.

Coronary angiography Coronary angiograms were acquired with Axiom Artis dFC (Siemens, Erlangen, Germany) and were analyzed offline using 2 contralateral projections for each artery before and after angioplasty, if applicable. All coronary segments were evaluated for the presence of visible myocardial bridge, epicardial slow-flow, thrombus in the epicardial artery, distal embolization during and after primary PCI, as well as the degree of stenosis based on visual inspection. In the patients with MI, epicardial blood flow in

the IRA was evaluated using the Thrombolysis in Myocardial Infarction (TIMI) scale.²⁸

Coronary artery wall pathology in optical coherence tomography Image acquisition All images were acquired with a commercially available system for OCT (Terumo, Tokyo, Japan). The OCT catheter was first advanced to the distal end of the IRA after aspiration thrombectomy followed by direct intracoronary injection of nitrates. The 80 mm long section of the IRA, including both the culprit lesion and adjacent to the culprit 10-mm proximal and distal segments, were then scanned using the integrated automated pullback device with a resolution of image acquisition of 158 frames/mm. During the image acquisition, coronary blood flow was replaced by continuous flushing of contrast media directly from the guiding catheter at a rate of 4 ml/s, with a power injector to create a virtually blood-free environment. Pullback was repeated after completing the PCI with a stent implantation. All images were recorded digitally, stored, and each frame was analyzed by an independent investigator blinded to the laboratory tests.

Image analysis An offline systematic analysis was performed using proprietary software after confirming calibration settings in frame-by-frame intervals separately for the culprit and adjacent non-culprit regions. The longitudinal view was used to identify the culprit lesion, and the adjacent to the culprit 10-mm proximal and 10-mm distal segment (Supplementary material, *Figure S1*).

Within the culprit lesion, its length, thrombus length, and the outlines of a lumen, the vessel, and the thrombus were contoured on each frame by multiple points trace function. Based on this contouring, the lumen area, the vessel area, the thrombus area, and the lesion area were calculated for each frame within the culprit lesion. The lesion volume was calculated as a mean difference between the vessel area and the lumen area multiplied by the lesion length, whereas the thrombus volume was calculated as a mean thrombus area multiplied by the thrombus length.^{29,30} In each case within the culprit lesion, the presence of TCFA including its rupture, necrotic core, macrophage infiltration, vasa vasorum, or intramural hematoma were assessed. The amount of lipid was expressed as a length of lipid-rich pool with an arc above 90 degrees, whereas the amount of calcium was expressed as a maximum arc, its length, and maximum thickness.

Within the non-culprit segment of the IRA, the contours of the lumen, intima layer, and media layer were drawn by multiple points trace function on the most proximal frame (IRA proximal reference [A]), on the most available distal frame (IRA distal reference [L]), on the 3 frames (10 mm before [B], 5 mm before [C], and at the proximal border of the culprit [D]) within the 10-mm adjacent

to the culprit lesion proximal segment, and on the other 3 frames (10 mm after [I], 5 mm after [J], and at the distal border of the culprit [K]) within the 10-mm distal adjacent segment. The obtained contours were used for the calculation of the areas of the intima, media, intima-media, lumen, and the vessel (Supplementary material, *Figure S1B1*). At the same frames, mean diameters of the intima, media, intima-media, lumen, and the vessel were calculated based on the measurements performed every 90 degrees (Supplementary material, *Figure S1B2*). Mean values for the adjacent non-culprit region were derived from all the measurements obtained from the 10-mm proximal and distal segments. At each analyzed frame, the type of atherosclerotic plaque or lesion was defined as lipid, fibrous, calcified, thick intima, or as a normal wall (Supplementary material, *Figure S1*). The external border of the medial layer was not available for delineation in 1.04% of all OCT frames.

Long-term clinical follow-up Data on death, recurrent MI, stroke confirmed by imaging, or unplanned PCI due to unstable angina were collected during the follow-up at the outpatient clinic, and all of them were included in the composite ischemic end point. The data were supplemented by an in-person or telephone interview with the patient, or in the case of death, the data were obtained through an immediate relative.

Statistical analysis The study was powered to have a 90% chance to demonstrate a 10% relative decrease of ornithine/arginine (O/A) ratio during the 6-month follow-up with a SD of 20%.^{26,27} In the entire group, 44 patients or more were required to demonstrate such a difference with a *P* value below 0.05, and 88 patients with a *P* below 0.001.

The statistical analyses were performed using the SPSS Statistics software (Version 25.0.0.2, IBM, Armonk, New York, United States). Continuous variables were expressed as a median (interquartile range), whereas categorical variables were shown as a number (percentage). Continuous variables were first checked for a normal distribution with the Shapiro–Wilk test, and differences between the MI group and the controls were compared by the *t* test when normally distributed or by the Mann–Whitney test for non-normally distributed variables. Both normally and non-normally distributed dependent variables in the MI group were compared by the *t* test for paired samples or the Wilcoxon signed-rank test, respectively. In the MI group, relative changes between the acute MI phase and the follow-up for mean values of arginine metabolites and their ratios were calculated. Categorical variables were compared by the Fisher exact test. The Pearson or Spearman rank correlation coefficients were calculated to test the association between 2 variables with normal or non-normal distribution, respectively. Receiver operating characteristic (ROC) curves and the

Youden index were used to determine the optimal cutoff value for arginine metabolites and their indices in the prediction of the presence of TCFA within the culprit lesion or a composite ischemic end point during the follow-up. All independent variables potentially associated with both the exposure and outcome were included in the multivariable logistic regression to determine predictors of the presence of TCFA, or included in the multivariable linear regression to find parameters independently associated with the thickness of the coronary artery intima and intima-media. A 2-tailed *P* value below 0.05 was considered significant.

RESULTS Baseline characteristics More than 75% of the patients with MI were men and almost half of them had the anterior wall STEMI (**TABLE 1**). Most patients were in Killip class 1 on admission, and almost one-third of them had DM. The median time of ischemia was 121 (interquartile range [IQR], 90–309) minutes. At the first contrast injection, 35 patients had a TIMI-2/3 flow in the IRA, while following the procedure a TIMI-3 flow was achieved in 96 patients. The controls were less likely to smoke than the MI patients, and were treated less frequently with aspirin, statins, and β -blockers, but more often with calcium channel blockers. On coronary angiography, 10 controls had tortuous epicardial segments, and 8 had a myocardial bridge.

Altered balance of arginine metabolites in the acute and stable myocardial infarction phase Following ischemia, the median concentration of ornithine was higher by 73% and of proline by 76%, the level of arginine was lower by 41%, ADMA by 40%, MMA by 24%, and citrulline by 71% (*P* < 0.001 for all) (**FIGURE 1**), when compared with the stable condition after 6 months. As compared with the stable phase of MI, the controls had lower levels of ornithine (*P* < 0.001), proline (*P* = 0.004), and ADMA (*P* = 0.006) without significant differences in arginine (*P* = 0.35) and citrulline (*P* = 0.61) (**FIGURE 1**).

In the acute phase of MI, the citrulline/arginine (C/A) and citrulline/ornithine (C/O) ratios, and GABR were lower, while O/A and proline/arginine (P/A) ratios were higher than after 6 months (*P* < 0.001 for all). As compared with the stable phase of MI, the controls had lower O/A (*P* = 0.02) and P/A (*P* = 0.02) ratios, higher C/O ratio (*P* = 0.002), and showed no significant differences in GABR (*P* = 0.13), C/A ratio (*P* = 0.10) (**FIGURE 1**), arginine/ADMA (*P* = 0.66) ratio, and P/O ratio (*P* = 0.18). There were significant correlations between arginine metabolites at both time points (Supplementary material, *Table S1*).

Arginine metabolites and clinical characteristics, lipid profile, inflammatory biomarkers and medications At baseline, the concentrations of arginine metabolites and their indices were not associated with body mass index, the time of

TABLE 1 Baseline and in-hospital characteristics

Parameter	MI patients (n = 100)	Controls (n = 25)	P value
Age, y	62 (54–69)	64 (60–69)	0.17
Male sex	78 (78)	18 (72)	0.30
Body mass index, kg/m ²	27.6 (25.2–31)	28.5 (26.3–31.9)	0.66
Anterior wall myocardial infarction	49 (49)	–	–
Killip class >1 on admission	5 (5)	–	–
Cardiovascular risk factors			
Hypertension	79 (79)	22 (88)	0.40
Diabetes mellitus	30 (30)	5 (20)	0.46
Dyslipidemia	68 (68)	21 (84)	0.14
Smoking	52 (52)	4 (16)	0.004
Family history of coronary artery disease	42 (42)	10 (40)	0.98
Comorbidities			
Prior myocardial infarction	9 (9)	0	0.20
Prior percutaneous coronary intervention	6 (6)	0	0.60
History of stroke	3 (3)	1 (4)	0.36
History of peripheral vascular disease	1 (1)	0	0.99
Chronic kidney disease	6 (6)	1 (4)	0.99
Baseline laboratory results			
Hemoglobin, g/dl	15.1 (14.1–16)	14.4 (13.4–14.9)	0.11
Hematocrit, %	44.2 (42–47.1)	43 (40.5–44.6)	0.09
Platelets, × 10 ³ /μl	235 (203–283)	232 (191–246)	0.21
White blood cells, × 10 ³ /μl	10.1 (8.3–13.1)	6.0 (5.7–7.4)	<0.001
Glucose, mmol/l	8.2 (7–10)	5.4 (5.2–6.1)	<0.001
Creatinine, μmol/l	84 (75–93)	76 (63–93)	0.19
hsCRP, mg/l	2.21 (1.08–3.64)	1.95 (0.78–2.33)	0.23
Fibrinogen, g/l	3.53 (3.16–3.99)	3.21 (2.95–4.1)	0.67
Total cholesterol, mmol/l	5.28 (4.52–6.23)	4.71 (4.16–5)	0.007
LDL cholesterol, mmol/l	3.6 (2.96–4.34)	2.78 (2.20–3.45)	<0.001
HDL cholesterol, mmol/l	1.27 (1.06–1.56)	1.45 (1.10–1.78)	0.12
Triglycerides, mmol/l	1.68 (1.01–2.54)	1.50 (1.20–2.19)	0.34
Troponin T, ng/ml	0.087 (0.022–0.284)	–	–
Isoenzyme MB of creatine kinase, IU/l	21 (16–38.5)	–	–
Antithrombotic treatment before admission			
Aspirin, loading dose of 300 mg p.o.	100 (100)	–	–
Ticagrelor, loading dose of 180 mg p.o.	75 (75)	–	–
Clopidogrel, loading dose of 600 mg p.o.	25 (25)	–	–
Treatment at discharge			
Aspirin	98 (98)	21 (84)	0.02
Clopidogrel	10 (10)	–	–
Ticagrelor	86 (86)	–	–
Prasugrel	4 (4)	–	–
ACEI or ARB	88 (88)	18 (72)	0.07
β-Blocker	97 (97)	17 (68)	<0.001
Calcium channel blocker	9 (9)	10 (40)	0.009
Statin	97 (97)	20 (80)	0.008

Data are shown as median (interquartile range) or number (percentage).

Conversion factors: to convert hemoglobin to mmol/l, multiply by 0.6206, hsCRP to nmol/l, multiply by 9.5238, troponin T to μg/l, multiply by 1

Abbreviations: ACEI, angiotensin-converting enzyme inhibitors; ARB, angiotensin receptor blockers; LDL, low-density lipoprotein; HDL, high-density lipoprotein; hsCRP, high-sensitivity C-reactive protein; p.o., per os

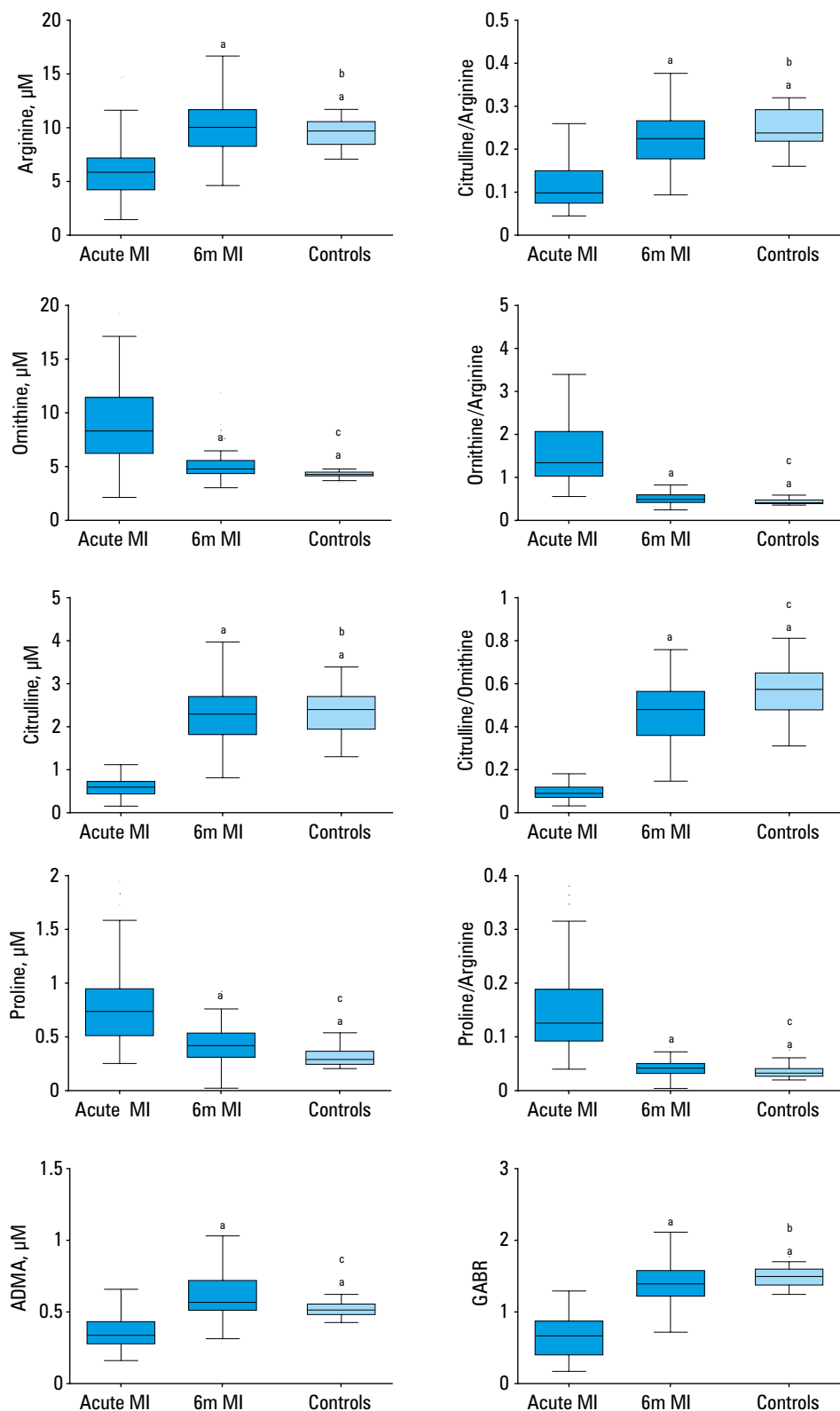


FIGURE 1 Arginine metabolites and their indices in the compared groups. Box plots show median and interquartile range (IQR) (Q3–Q1). Q1 and Q3 are the first and third quartiles. Whiskers are drawn at $Q3 + 1.5 \times \text{IQR}$, $Q1 - 1.5 \times \text{IQR}$. Extreme values are omitted.

a $P < 0.001$ vs acute MI

b $P \geq 0.05$ vs 6m MI

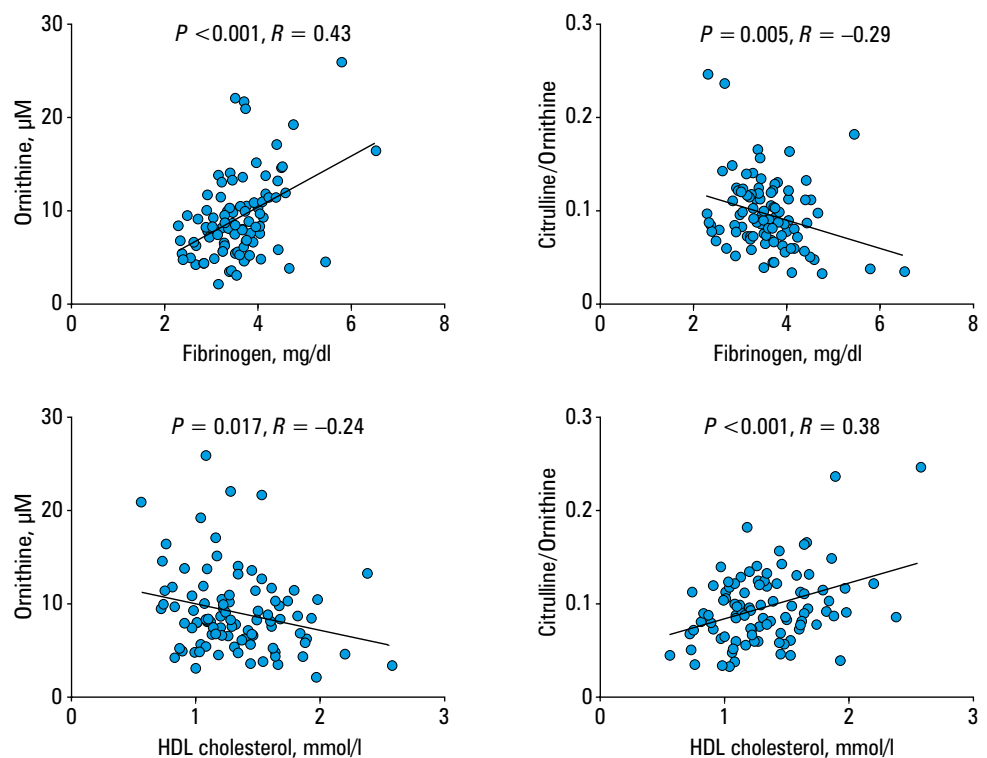
c $P < 0.05$ vs 6m MI

Abbreviations: 6m MI, 6 months after MI; acute MI, acute phase of myocardial infarction; ADMA, asymmetric dimethylarginine; GABR, global arginine bioavailability ratio

ischemia, loading dose of clopidogrel, ticagrelor or prasugrel, hsCRP or TIMI flow in the IRA

before and after PCI. However, plasma fibrinogen correlated positively with ornithine ($R = 0.43$;

FIGURE 2 Arginine metabolites, their indices vs traditional cardiovascular biomarkers measured in the acute phase of myocardial infarction. Abbreviations: *R*, correlation coefficient; others, see **TABLE 1**. Conversion factors: see **TABLE 1**.



$P < 0.001$), O/A ratio ($R = 0.23$; $P = 0.03$) and negatively with C/O ratio ($R = -0.29$; $P = 0.005$) (**FIGURE 2**). In contrast, high-density lipoprotein cholesterol correlated positively with C/O ratio ($R = 0.38$; $P < 0.001$) and negatively with plasma ornithine ($R = -0.24$; $P = 0.02$). There were no differences in arginine metabolite profile at both time points between the patients treated with atorvastatin ($n = 57$) vs rosuvastatin ($n = 40$). In controls, triglyceride concentration negatively correlated with arginine ($R = -0.42$; $P = 0.04$) and citrulline ($R = -0.60$; $P = 0.005$), while total cholesterol positively correlated with ornithine ($R = 0.40$; $P = 0.045$).

Arginine metabolites and thin-cap fibroatheroma

OCT findings are shown in **TABLE 2**. The patients with TCFA present in the IRA culprit lesion in an acute phase had higher plasma levels of ADMA ($P = 0.02$), MMA ($P = 0.03$), and ornithine ($P = 0.003$) without changes in the concentration of arginine, citrulline, or proline (**FIGURE 3**). Simultaneously, the C/O ratio ($P = 0.003$) and the arginine/ADMA ratio ($P = 0.04$) were lower, and the O/A ratio was higher ($P = 0.045$) in the patients with TCFA than in those without TCFA. The patients with TCFA were characterized by higher plasma hsCRP (2.28 [IQR, 1.08–3.68] vs 1.23 [IQR, 0.71–2.10] mg/dl; $P = 0.02$) and creatinine (86 [IQR, 76–95] vs 78 [IQR, 69–86] μ M; $P = 0.009$), and more frequent DM (36% vs 12%; $P = 0.03$) than the patients without TCFA. Moreover, the length of the lipid-rich pool correlated with the proline level on admission ($R = 0.24$; $P = 0.03$). Also, in the acute phase, hsCRP correlated with the volume of the culprit lesion ($R = 0.25$; $P = 0.04$).

Arginine metabolites and intima-media of the non-culprit infarct-related artery segment

A mean diameter of the intima or intima-media in the adjacent segment of the IRA was higher in men than in women (Supplementary material, *Table S2*), and after 6 months correlated positively with the O/A ratio and negatively with arginine concentration, GABR, and the C/O ratio (Supplementary material, *Table S3*). Also, a mean diameter of the intima and intima-media of the distal IRA reference segment correlated positively with the 6-month O/A ratio and negatively with the concentrations of arginine, proline, citrulline, and C/O and P/A ratios. A mean diameter of the media in the distal IRA reference segment inversely correlated with the follow-up levels of arginine, citrulline, proline, and C/O ratio. The more distal the analyzed segment, the stronger were the correlations between the diameters of the intima, intima-media, media, and arginine metabolites and their indices. Analogous associations for the areas of the intima or intima-media are shown in Supplementary material, *Table S3*.

Determinants of thin-cap fibroatheroma presence or the adjacent non-culprit intima-media burden

Before inclusion in the multivariable models, all significant associations between independent covariates were identified. Age negatively correlated with the hemoglobin level ($R = -0.29$; $P = 0.01$) and the median plasma creatinine was higher by 19% ($P = 0.003$) in men than in women. The patients with DM had by 11% ($P = 0.02$) higher median concentration of creatinine and by 45% ($P = 0.023$) higher levels of hsCRP.

In the multivariable logistic regression, a higher baseline creatinine level ($P = 0.03$) and

TABLE 2 The infarct-related artery characteristics in the optical coherence tomography

Culprit lesion		Non-culprit segment of the IRA			
Parameter	Value	Parameter	Proximal	Adjacent ^a	Distal
Vessel volume, mm ³	329 (237–441)	Area, mm ²			
Lumen volume, mm ³	106 (77–156)	Vessel	19.8 (16.5–23.8)	15.1 (12.0–18.1)	7.7 (5.9–9.9)
Lesion volume, mm ³	219 (150–310)	Lumen	11.3 (9.2–15.3)	7.7 (6.1–9.5)	4.1 (3.0–5.4)
Thrombus volume, mm ³	2.0 (0.5–5.1)	Intima	5.9 (3.8–8.2)	4.9 (3.6–6.5)	2.0 (1.0–3.3)
Lesion length, mm	22.5 (17.1–29.4)	Media	2.0 (1.7–2.3)	1.7 (1.4–2.0)	1.0 (0.7–1.4)
Minimum lumen area, mm ²	1.1 (0.8–1.4)	Intima-media	7.8 (5.8–10.4)	6.7 (5.3–8.2)	3.1 (1.8–4.5)
The cause of IRA occlusion		Area as a ratio of the vessel area			
Plaque rupture	30 (30)	Lumen	0.60 (0.51–0.71)	0.55 (0.48–0.60)	0.59 (0.49–0.69)
Plaque erosion	49 (49)	Intima	0.28 (0.18–0.40)	0.33 (0.28–0.40)	0.26 (0.19–0.37)
Spontaneous dissection	14 (14)	Media	0.09 (0.08–0.11)	0.12 (0.10–0.13)	0.13 (0.12–0.16)
Tight stenosis	7 (7)	Intima-media	0.40 (0.29–0.49)	0.44 (0.39–0.52)	0.41 (0.31–0.51)
Necrotic core	49 (49)	Mean diameter, mm			
Macrophage infiltration	88 (88)	Vessel	5.02 (4.59–5.50)	4.30 (3.90–4.77)	3.13 (2.74–3.55)
Vasa vasorum	36 (36)	Lumen	3.81 (3.44–4.41)	3.09 (2.71–3.42)	2.28 (1.96–2.61)
Intramural hematoma	30 (30)	Intima	0.42 (0.30–0.67)	0.47 (0.34–0.58)	0.25 (0.16–0.39)
Thin-cap fibroatheroma	75 (78)	Media	0.12 (0.10–0.14)	0.13 (0.11–0.15)	0.10 (0.08–0.13)
Ruptured	44 (44)	Intima-media	0.55 (0.41–0.78)	0.62 (0.46–0.72)	0.38 (0.24–0.52)
Non-ruptured	31 (31)	Mean diameter as a ratio of vessel mean diameter			
Lipid-rich pool lesion	81 (81)	Lumen	0.78 (0.71–0.84)	0.73 (0.68–0.77)	0.77 (0.69–0.83)
Length of lipid-rich pool	12.3 (7.9–17.0)	Intima	0.08 (0.06–0.13)	0.11 (0.09–0.13)	0.08 (0.06–0.12)
Calcified lesion	35 (35)	Media	0.023 (0.021–0.030)	0.030 (0.027–0.034)	0.036 (0.03–0.042)
Maximum arcus, °	136 (109–202)	Intima-media	0.12 (0.08–0.16)	0.14 (0.12–0.16)	0.12 (0.09–0.16)
Maximum length, mm	4.8 (2.9–8.8)				
Maximum thickness, mm	0.92 (0.75–1.19)				
Dominant component of the culprit lesion		Dominant type of the non-culprit lesion			
Thrombus	18 (18)	Thick intima	5 (5)	6 (6)	7 (7)
Lipid	54 (54)	Lipid	40 (40)	50 (50)	12 (12)
Fibrous lesion	19 (19)	Fibrous lesion	11 (11)	28 (28)	36 (36)
Calcified lesion	9 (9)	Calcified lesion	6 (6)	5 (5)	1 (1)
		Normal segment	36 (36)	11 (11)	44 (44)

Data are shown as median (interquartile range) or number (percentage).

a Mean values calculated for all measurements performed within 10-mm segments adjacent proximally and distally to the culprit lesion

Abbreviations: IRA, infarct-related artery

a lower baseline C/O ratio ($P = 0.006$) influenced the presence of TCFA in the culprit lesion (TABLE 3). The C/O ratio reached the area under the ROC curve of 0.77 (95% CI, 0.66–0.88) for prediction of TCFA with a cutoff value equal to or below 0.12, and sensitivity of 89% and specificity of 57.1% (Supplementary material, Figure S2A).

Simultaneously, in the multivariable analysis, male sex ($P < 0.001$), DM ($P = 0.02$), and a higher 6-month O/A ratio ($P = 0.02$) were independently associated with a higher mean intima-media diameter in the adjacent IRA segment. The same predictors independently influenced the mean intima diameter in a similar way (TABLE 3).

A signal of long-term clinical outcomes Of 100 MI patients, within the median follow-up of 23 (IQR, 16–35) months, 4 patients died, including 2

before discharge, recurrent MI occurred in 4 survivors, stroke occurred in 3 patients, and unplanned PCI due to unstable angina was performed in further 3 patients. The composite ischemic end point was found in 14 patients. Of all the arginine metabolites and their metabolic indices, follow-up GABR was lower, while O/A ratio was higher in the patients with vs without the ischemic composite end point (Supplementary material, Table S4). The follow-up O/A ratio reached the area under the ROC curve of 0.80 (95% CI, 0.68–0.91) for prediction of the composite ischemic end point with a cutoff value equal to or above 0.57, and sensitivity of 74.1% and specificity of 78.0% (Supplementary material, Figure S2B).

DISCUSSION The current study is the first to demonstrate that a shift in arginine metabolism

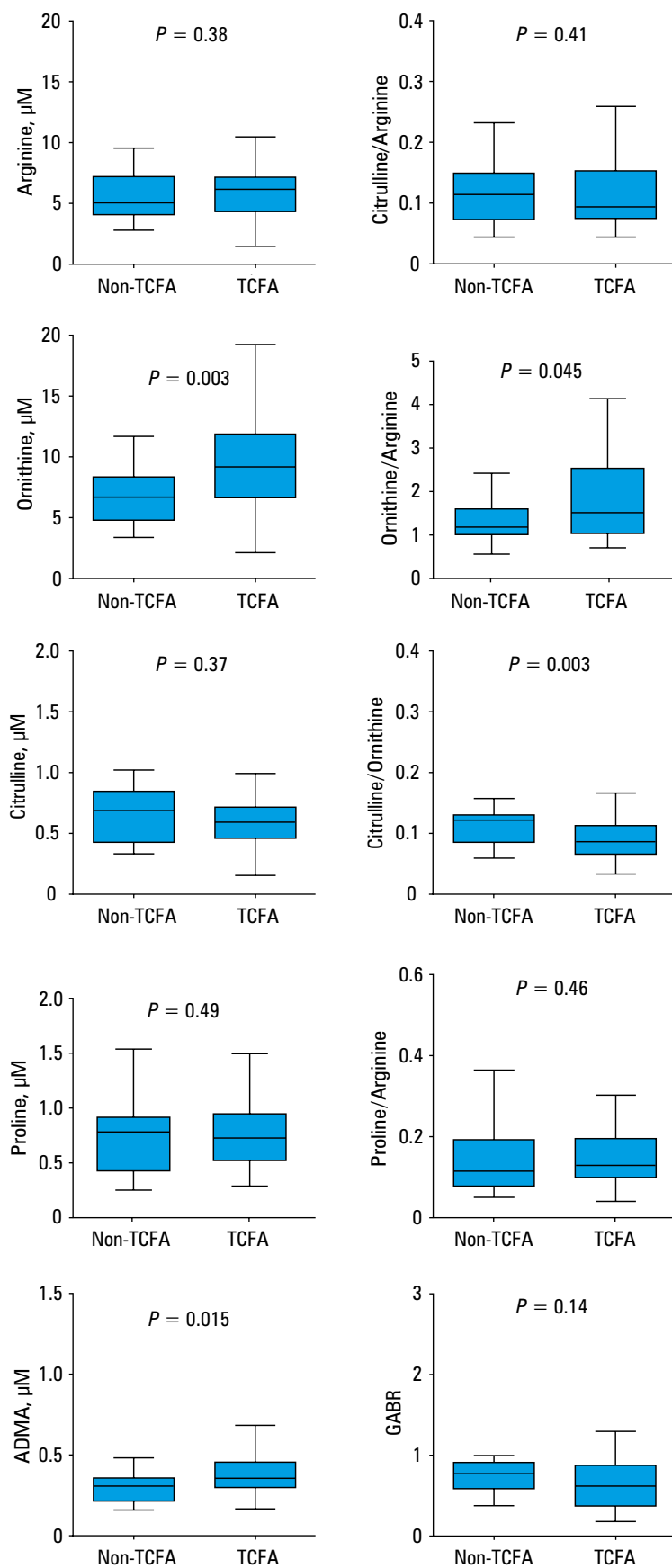


FIGURE 3 Arginine metabolites and their indices in the patients with and without TCFA. Box plots show median and interquartile range (IQR) (Q3–Q1). Q1 and Q3 are the first and third quartiles. Whiskers are drawn at $Q3 + 1.5 \times \text{IQR}$, $Q1 - 1.5 \times \text{IQR}$. Extreme values are omitted.

Abbreviations: TCFA, thin-cap fibroatheroma; others, see [FIGURE 1](#)

toward the pathway catalyzed by arginase instead of NOS in the acute phase of MI is associated with the presence of TCFA in the culprit region of IRA ([FIGURE 4](#)). During the stable chronic phase in patients receiving optimal pharmacotherapy, analogous persistent alterations correlate both with the size of the intima or intima-media in the adjacent non-culprit segment of IRA. After adjustment for clinical characteristics, the parameters of the arginine metabolites balance both in the acute and chronic phase were found to be independent predictors of the structure of the culprit and non-culprit IRA regions, respectively. Our findings suggest that an altered balance of arginine metabolites might be considered as an indicator of the presence of a vulnerable plaque as well as of the extent of the atherosclerotic burden in the IRA segment adjacent to the culprit lesion.

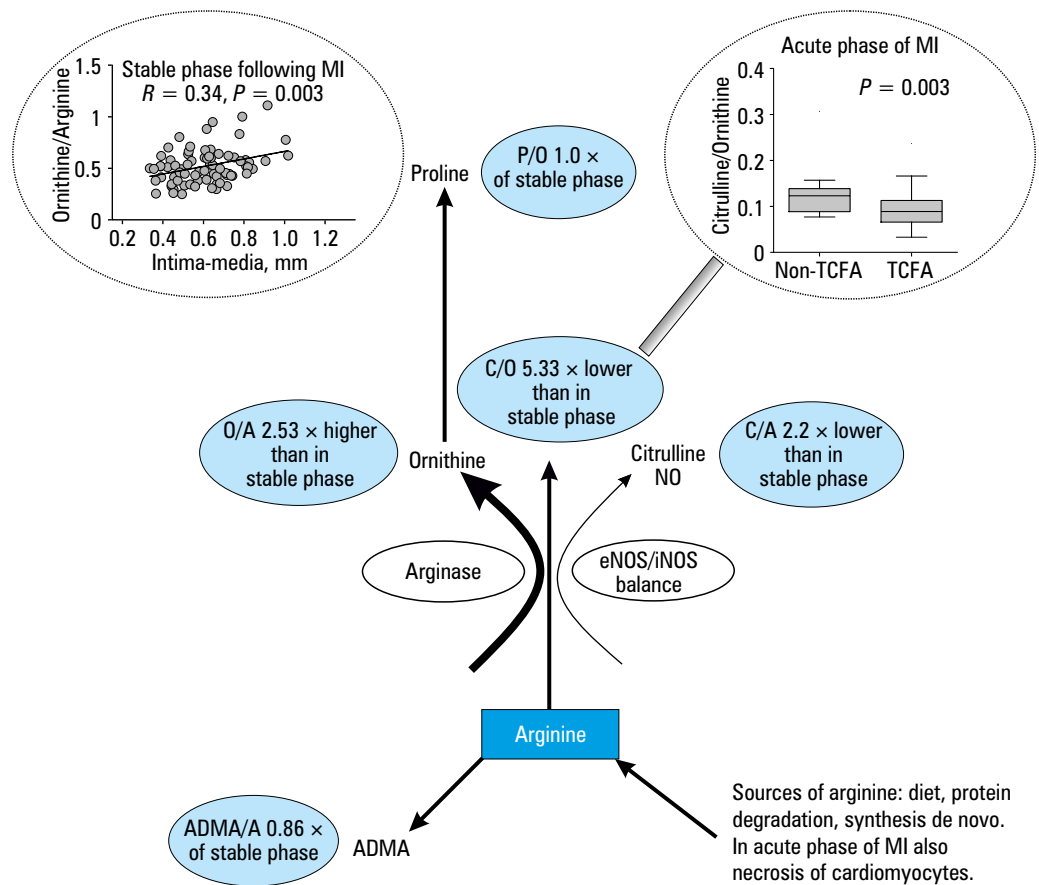
The experimental studies indicate that the expression of arginase-1 in ischemic and reperfused myocardium is higher than in the remote region³¹ and is associated with an increased vascular production of superoxide anion and/or decreased endothelial levels of tetrahydrobiopterin or L-arginine resulting in diminished NO synthesis.^{32,33} Increased arginase expression after ischemia/reperfusion was also found in coronary artery endothelial cells and vascular smooth muscle cells.^{26,34} Our current and previous²⁷ clinical findings are in line with the experimental studies and provide indirect but consistent arguments for a relatively enhanced activation of arginase over NOS in the patients with acute MI. In a rat model of myocardial ischemia/reperfusion, Schreckenberget al³⁵ demonstrated that enhanced arginase activity, initially triggered by endothelial NOS uncoupling, starts within 2 hours of reperfusion, and is maintained by tumor necrosis factor α -dependent induction of arginase-1 and downregulation of endothelial NOS. Apart from arginase overexpression, endothelial NOS uncoupling and increased activation of inducible NOS in the acute phase of MI must be considered when describing the shift in L-arginine utilization^{1,5} ([FIGURE 4](#)).

A fragile TCFA within a coronary plaque prone to rupture, erosion, or ulceration is a trigger for thrombus formation.^{36,37} Plaque vulnerability associated with a vascular smooth muscle cell apoptosis induced by arginase-2 was found in a cell culture model as well as in atherosclerosis-prone apolipoprotein E-deficient mice.³⁸ In mice, increased carotid arginase activity was associated with enhanced shear stress, and newly formed atherosclerotic plaques had a vulnerable-like phenotype with a decreased number of smooth muscle cells, lower collagen content, and higher content of macrophages and lipids.³⁹ Keeping in mind all the limitations associated with in vitro studies and in vivo animal models, we have shown for the first time in humans that the presence of a TCFA in the culprit lesion is associated with a shift of arginine metabolism toward arginase, expressed as an increased O/A ratio and decreased

TABLE 3 Independent predictors of the presence of thin-cap fibroatheroma in the culprit lesion and of the thickness of intima or intima-media in the adjacent to the culprit region

Independent variables	Univariable model			Multivariable model		
	OR	P value	95% CI for OR	OR	P value	95% CI for OR
Presence of TCFA in the culprit lesion, Nagelkerke $R^2 = 0.29$, $P < 0.001$						
Diabetes mellitus, yes vs no	3.891	0.04	1.050–14.286	3.086	0.12	0.75–12.658
Creatinine, per 1 $\mu\text{mol/l}$	1.048	0.02	1.009–1.089	1.049	0.03	1.004–1.096
Citrulline/ornithine, per 0.01	0.979	0.005	0.965–0.994	0.978	0.006	0.962–0.994
Mean intima-media diameter of the adjacent segment, $R^2 = 0.39$, $P < 0.001$						
	β	P value	95% CI for β	β	P value	95% CI for β
Age, per 1 year	0.218	0.03	0.017–0.412	0.197	0.05	–0.002 to 0.394
Male sex, no vs yes	0.313	0.002	0.118–0.508	0.399	<0.001	0.212–0.585
Diabetes mellitus, no vs yes	0.293	0.004	0.095–0.491	0.222	0.02	0.03–0.414
Ornithine/arginine, per 0.01	0.337	0.003	0.112–0.561	0.227	0.02	0.045–0.409
Mean intima diameter of the adjacent segment, $R^2 = 0.35$, $P < 0.001$						
	β	P value	95% CI for β	β	P value	95% CI for β
Age, per 1 year	0.079	0.18	–0.021 to 0.383	0.175	0.08	–0.023 to 0.373
Male sex, no vs yes	0.353	<0.001	0.160–0.546	0.434	<0.001	0.247–0.620
Diabetes mellitus, no vs yes	0.264	0.01	0.064–0.464	0.203	0.04	0.012–0.394
Ornithine/arginine, per 0.01	0.291	0.009	0.085–0.497	0.218	0.02	0.036–0.412

Abbreviations: β , coefficient; OR, odds ratio; others, see **FIGURE 3**



C/O ratio following ischemia. Although expected, there were no differences in baseline proline levels between the patients with and without

TCFA, likely due to high plasma proline amounts released from the disrupted cardiomyocytes in the acute phase of MI.

Looking for accurate, noninvasive, and reproducible biomarkers of atherosclerosis progression, including its asymptomatic and very early stages associated with endothelial dysfunction, is of clinical importance.⁴⁰ Previous studies showed that during 9 to 18 months of observation, regression of the atherosclerotic plaque associated with potent lipid-lowering therapy was low and reached less than 2.2% of the baseline volume.²⁰⁻²⁵ Therefore, we compared the baseline OCT findings with a 6-month profile of arginine metabolites. In the patients without any adverse cardiac ischemic events during the follow-up, persistent metabolic shift toward arginase correlated with increased thickness of the coronary intima or intima-media complex in the adjacent non-culprit segments of the IRA. Arginase as a source of polyamines and L-proline promotes intimal hyperplasia and coronary artery remodeling.⁴¹ In contrast, arginase inhibition leads to a significant decline in the number of vascular smooth muscle cells, DNA synthesis, and reduced intimal thickening.⁴² Previous studies showed an association between greater intima-media thickness and an increased endothelial cell concentration of NOS inhibitors,⁴³ or enhanced arginase activity.⁴⁴ A preserved endothelial function, as measured by flow-mediated dilatation, inversely correlated with the plasma ADMA and hsCRP concentration.⁴⁵ Future studies on the role of genetic background for arginase functioning are needed to establish causal relevance of these potential pathways.⁴⁶ This study provides a clinical signal for potential reevaluation of existing arginase inhibitors as well as for development of novel therapeutic molecules interfering with arginine metabolism in the treatment of MI patients.

This study has several limitations. First, the analyzed group was of a medium size, although the sample size was calculated based on rigorous assumptions derived from meticulously measured OCT parameters and arginine metabolites. Second, arginine as well as NO metabolites⁴⁷ were not measured in the acute phase following reperfusion. Third, our results have limited predictive clinical value due to the small number of end points observed during the follow-up, even though this study was not powered for clinical events.^{48,49} Finally, as majority of the patients were treated with statins or angiotensin-converting enzyme inhibitors/angiotensin receptor blockers, we could not assess the effect of lipid-lowering or blood pressure-lowering therapy on the arginine metabolites profile.

In conclusion, our findings show that during the acute phase of MI, arginine metabolism is shifted from NOS toward arginase, as compared with stable conditions. Simultaneously, our results suggest that enhanced arginase activity upon admission is associated with the presence of TCFA in the culprit lesion and might indicate patients who are more likely to have vulnerable plaque, while a similar residual metabolic shift in the chronic phase correlates with the thickness of

intima-media in the segment adjacent to the culprit IRA. These new indices derived from arginine metabolism might be useful as indicators of acute and chronic features of atherosclerosis, although their validation in a larger cohort focusing on clinical additive utility to standard risk variables, as well as the impact of lifestyle, diet, and medical therapy of these measures, is required.

SUPPLEMENTARY MATERIAL

Supplementary material is available at www.mp.pl/paim.

ARTICLE INFORMATION

ACKNOWLEDGMENTS None.

FUNDING This work was supported by the grant from the National Science Center of Poland (2016/21/B/NZ5/01378 to JZ).

CONTRIBUTION STATEMENT PM and JZ contributed to the concept and design of the study. All authors were involved in data collection. JZ analyzed the data and coordinated funding. All authors edited and approved the final version of the manuscript.

CONFLICT OF INTEREST None declared.

OPEN ACCESS This is an Open Access article distributed under the terms of the Creative Commons Attribution-NonCommercial-ShareAlike 4.0 International License (CC BY-NC-SA 4.0), allowing third parties to copy and redistribute the material in any medium or format and to remix, transform, and build upon the material, provided the original work is properly cited, distributed under the same license, and used for noncommercial purposes only. For commercial use, please contact the journal office at pamw@mp.pl.

HOW TO CITE Motek P, Żmudzki P, Machnik A, et al. Thin-cap fibroatheroma and increased coronary intima-media thickness are associated with an altered arginine metabolites balance. *Pol Arch Intern Med.* 2023; 133: 16356. doi:10.20452/pamw.16356

REFERENCES

- 1 Cyr AR, Huckaby LV, Shiva SS, Zuckerbraun BS. Nitric oxide and endothelial dysfunction. *Crit Care Clin.* 2020; 36: 307-321. [↗](#)
- 2 Deanfield JE, Halcox JP, Rabelink TJ. Endothelial function and dysfunction: testing and clinical relevance. *Circulation.* 2007; 115: 1285-1295. [↗](#)
- 3 Morris SM Jr. Arginine metabolism revisited. *J Nutr.* 2016; 146: 2579S-2586S. [↗](#)
- 4 Caldwell RW, Rodriguez PC, Toque HA, et al. Arginase: a multifaceted enzyme important in health and disease. *Physiol Rev.* 2018; 98: 641-665. [↗](#)
- 5 Förstermann U, Sessa WC. Nitric oxide synthases: regulation and function. *Eur Heart J.* 2012; 33: 829-837. [↗](#)
- 6 Imiela T, Imiela AM, Karczmarewicz G, Budaj A. Acidic urine as a novel risk factor for diuretic resistance and worse in-hospital prognosis in patients with acute heart failure. *Pol Arch Intern Med.* 2021; 131: 16054. [↗](#)
- 7 Vichova T, Waldauf P, Karpisek M, et al. Oxidative stress markers, thio-redoxin 1 and 8-isoprostane, in relation to ischemic time in patients with ST-segment elevation myocardial infarction treated by primary percutaneous coronary intervention. *Pol Arch Intern Med.* 2021; 131: 755-758. [↗](#)
- 8 Simsek B, Cinar T, Tank VO, et al. The association of acute-to-chronic glycemic ratio with no-reflow in patients with ST-segment elevation myocardial infarction undergoing primary percutaneous coronary intervention. *Kardiol Pol.* 2021; 79: 170-178. [↗](#)
- 9 Tabas I, Williams KJ, Boren J. Subendothelial lipoprotein retention as the initiating process in atherosclerosis: update and therapeutic implications. *Circulation.* 2007; 116: 1832-1844. [↗](#)
- 10 Libby P, Lichtman AH, Hansson GK. Immune effector mechanisms implicated in atherosclerosis: from mice to humans. *Immunity.* 2013; 38: 1092-1104. [↗](#)
- 11 Ridker PM. A test in context: high-sensitivity C-reactive protein. *J Am Coll Cardiol.* 2016; 67: 712-723. [↗](#)
- 12 Möhlenkamp S, Lehmann N, Moebus S, et al. Quantification of coronary atherosclerosis and inflammation to predict coronary events and all-cause mortality. *J Am Coll Cardiol.* 2011; 57: 1455-1464. [↗](#)
- 13 Terlecki M, Kocowska-Trytko M, Plens K, et al. Prognostic value of acid-base balance parameters assessed on admission in peripheral venous blood of patients with myocardial infarction treated with percutaneous coronary intervention. *Pol Arch Intern Med.* 2022; 132: 16229. [↗](#)
- 14 Cao J, Hsu Y-H, Li S, et al. Lipoprotein-associated phospholipase A(2) interacts with phospholipid vesicles via a surface-disposed hydrophobic alpha-helix. *Biochemistry.* 2011; 50: 5314-5321. [↗](#)
- 15 Mittal EB, Mishra A, Srivastava A, et al. Matrix metalloproteinases in coronary artery disease. *Adv Clin Chem.* 2014; 64: 1-72. [↗](#)
- 16 Ndrepepa G, Braun S, Mehilli J, et al. Myeloperoxidase level in patients with stable coronary artery disease and acute coronary syndromes. *Eur J Clin Invest.* 2008; 38: 90-96. [↗](#)

- 17 Dong L, Mintz GS, Witzenschnicker B, et al. Comparison of plaque characteristics in narrowings with ST-elevation myocardial infarction (STEMI), non-STEMI/unstable angina pectoris and stable coronary artery disease (from the ADAPT-DES IVUS Substudy). *Am J Cardiol.* 2015; 115: 860-866. [↗](#)
- 18 Gili S, Iannaccone M, Colombo F, et al. Effects of statins on plaque rupture assessed by optical coherence tomography in patients presenting with acute coronary syndromes: insights from the optical coherence tomography (OCT)-FORMIDABLE registry. *Eur Heart J Cardiovasc Imaging.* 2018; 19: 524-531. [↗](#)
- 19 Homorodean C, Leucuta DC, Ober M, et al. Intravascular ultrasound insights into the unstable features of the coronary atherosclerotic plaques: a systematic review and meta-analysis. *Eur J Clin Invest.* 2022; 52: e13671. [↗](#)
- 20 Hou J, Xing L, Jia H, et al. Comparison of intensive versus moderate lipid lowering therapy on fibrous cap and atheroma volume of coronary lipid rich plaque using serial optical coherence tomography and intravascular ultrasound imaging. *Am J Cardiol.* 2016; 117: 800-806. [↗](#)
- 21 Råber L, Koskinas KC, Yamaji K, et al. Changes in coronary plaque composition in patients with acute myocardial infarction treated with high intensity statin therapy (IBIS 4): a serial optical coherence tomography study. *JACC Cardiovasc Imaging.* 2019; 12: 1518-1528. [↗](#)
- 22 Yano H, Horinaka S, Ishimitsu T. Effect of evolocumab therapy on coronary fibrous cap thickness assessed by optical coherence tomography in patients with acute coronary syndrome. *J Cardiol.* 2020; 75: 289-295. [↗](#)
- 23 Råber L, Ueki Y, Otsuka T, et al. Effect of aliocumab added to high-intensity statin therapy on coronary atherosclerosis in patients with acute myocardial infarction: the PACMAN-AMI randomized clinical trial. *JAMA.* 2022; 3: e225218. [↗](#)
- 24 Tsujita K, Sugiyama S, Sumida H, et al. Impact of dual lipid-lowering strategy with ezetimibe and atorvastatin on coronary plaque regression in patients with percutaneous coronary intervention: the multicenter randomized controlled PRECISE-IVUS Trial. *J Am Coll Cardiol.* 2015; 66: 495-507.
- 25 Nicholls SJ, Puri R, Anderson T, et al. Effect of evolocumab on coronary plaque composition. *J Am Coll Cardiol.* 2018; 72: 2012-2021. [↗](#)
- 26 Jung C, Gonon AT, Sjöquist PO, et al. Arginase inhibition mediates cardioprotection during ischaemia-reperfusion. *Cardiovasc Res.* 2010; 85: 147-154. [↗](#)
- 27 Molek P, Zmudzki P, Włodarczyk A, et al. The shifted balance of arginine metabolites in acute myocardial infarction patients and its clinical relevance. *Sci Rep.* 2021; 11: 83. [↗](#)
- 28 Zalewski J, Zmudka K, Musialek P, et al. Detection of microvascular injury by evaluating epicardial blood flow in early reperfusion following primary angioplasty. *Int J Cardiol.* 2004; 96: 389-396. [↗](#)
- 29 Sinclair H, Bourantas C, Bagnall A, et al. OCT for the identification of vulnerable plaque in acute coronary syndrome. *JACC Cardiovasc Imaging.* 2015; 8: 198-209. [↗](#)
- 30 Tearney GJ, Regar E, Akasaka T. Consensus standards for acquisition, measurement, and reporting of intravascular optical coherence tomography studies: a report from the International Working Group for Intravascular Optical Coherence Tomography Standardization and Validation. *J Am Coll Cardiol.* 2012; 59: 1058-1072.
- 31 Lefer AM, Tsao PS, Lefer DJ, et al. Role of endothelial dysfunction in the pathogenesis of reperfusion injury after myocardial ischemia. *FASEB J.* 1991; 5: 2029-2034. [↗](#)
- 32 Tiefenbacher CP, Chilian WM, Mitchell M, DeFily DV. Restoration of endothelium-dependent vasodilation after reperfusion injury by tetrahydrobiopterin. *Circulation.* 1996; 94: 1423-1429. [↗](#)
- 33 Weyrich AS, Ma X, Lefer AM. The role of L-arginine in ameliorating reperfusion injury after myocardial ischemia in the cat. *Circulation.* 1992; 86: 279-288. [↗](#)
- 34 Pernow J, Jung C. Arginase as a potential target in the treatment of cardiovascular disease: reversal of arginine steal? *Cardiovasc Res.* 2013; 98: 334-343. [↗](#)
- 35 Schreckenberg R, Weber P, Cabrera-Fuentes HA, et al. Mechanism and consequences of the shift in cardiac arginine metabolism following ischaemia and reperfusion in rats. *Thromb Haemost.* 2015; 113: 482-493. [↗](#)
- 36 Garcia-Garcia HM, Jang IK, Serruys PW, et al. Imaging plaques to predict and better manage patients with acute coronary events. *Circ Res.* 2014; 114: 1904-1917. [↗](#)
- 37 Iwańczyk S, Skorupski WJ, Kępski S, et al. Thromboembolic or atherosclerotic? Optical coherence tomography in determining the cause of myocardial infarction with ST-segment elevation. *Kardiol Pol.* 2020; 78: 1045-1046. [↗](#)
- 38 Xiong Y, Yu Y, Montani JP, et al. Arginase-II induces vascular smooth muscle cell senescence and apoptosis through p66Shc and p53 independently of its L-arginine ureahydrolase activity: implications for atherosclerotic plaque vulnerability. *J Am Heart Assoc.* 2013; 2: e000096. [↗](#)
- 39 Olivon VC, Fraga-Silva RA, Segers D, et al. Arginase inhibition prevents the low shear stress-induced development of vulnerable atherosclerotic plaques in ApoE^{-/-} mice. *Atherosclerosis.* 2013; 227: 236-243. [↗](#)
- 40 Almeida SO, Budoff M. Effect of statins on atherosclerotic plaque. *Trends Cardiovasc Med.* 2019; 29: 451-455. [↗](#)
- 41 Yang Z, Ming XF. Endothelial arginase: a new target in atherosclerosis. *Curr Hypertens Rep.* 2006; 8: 54-59. [↗](#)
- 42 Wei LH, Wu G, Morris SM Jr, et al. Elevated arginase I expression in rat aortic smooth muscle cells increases cell proliferation. *Proc Natl Acad Sci U S A.* 2001; 98: 9260-9264. [↗](#)
- 43 Peyton KJ, Ensenat D, Azam MA, et al. Arginase promotes neointima formation in rat injured carotid arteries. *Arterioscler Thromb Vasc Biol.* 2009; 29: 488-494. [↗](#)
- 44 Azuma H, Sato J, Hamasaki H, et al. Accumulation of endogenous inhibitors for nitric oxide synthesis and decreased content of L-arginine in regenerated endothelial cells. *Br J Pharmacol.* 1995; 115: 1001-1004. [↗](#)
- 45 Ishizaka M, Nagai A, Iwanaga M, et al. Possible involvement of enhanced arginase activity due to up-regulated arginases and decreased hydroxyarginine in accelerating intimal hyperplasia with hyperglycemia. *Vascul Pharmacol.* 2007; 47: 272-280. [↗](#)
- 46 Mangiacapra F, Conte M, Demartini C, et al. Relationship of asymmetric dimethylarginine (ADMA) with extent and functional severity of coronary atherosclerosis. *Int J Cardiol.* 2016; 220: 629-633. [↗](#)
- 47 Janssens SP, Bogaert J, Zalewski J, et al. NOMI investigators. Nitric oxide for inhalation in ST-elevation myocardial infarction (NOMI): a multicentre, double-blind, randomized controlled trial. *Eur Heart J.* 2018; 39: 2717-2725. [↗](#)
- 48 Jankowski P, Topór-Mądry R, Gąsior M, et al. Management and predictors of clinical events in 75 686 patients with acute myocardial infarction. *Kardiol Pol.* 2022; 80: 468-475. [↗](#)
- 49 Wojtyński B, Gierlotka M, Opolski G, et al. Observed and relative survival and 5-year outcomes of patients discharged after acute myocardial infarction: the nationwide AMI-PL database. *Kardiol Pol.* 2020; 78: 990-998. [↗](#)